Femtosecond laser ablation of metals: a molecular dynamics simulation study

Xuan Liu (刘 璇) and Yang Wang (王 扬)

Department of Mechanical & Automation, Harbin Institute of Technology, Harbin 150001

Received May 21, 2004

Using molecular dynamics (MD) methods combining with two-step radiation heating model, the mechanisms of ablation and the thermodynamic states at Ni surface under femtosecond laser irradiation are investigated. Simulation results show that the main mechanisms of ablation are evaporation and tensile stresses generated inside the target. The velocity of stress wave is predicted to be nearly equal to sound velocity. The rates of ablation at different fluences obtained from simulations are in good agreement with experimental data. Superheating phenomenon is also discovered.

OCIS codes: 020.0020, 140.7090, 310.3840.

Over the recent years, ultra-short pulsed laser, especially femtosecond laser, has been rapidly developed and become a powerful tool for ablation of metals. A study of the basic mechanism involved in femtosecond laser ablation of metals is of great importance in terms of optimizing the efficiency of laser micro-machining and minimizing laser-induced damage. However, it is difficult to elucidate such mechanism by experiments due to the complexity and diversity of the processes involved during laser irradiation. Molecular dynamics (MD) method has solved this problem and demonstrated its potential for the further investigation of the subject above-mentioned.

In this paper, MD method combined with two-step radiation heating model is used to study a 500-fs pulse laser at $\lambda = 248$ nm interacting with Ni. The laser energy absorption and the thermal transport sustained by free electrons, and the energy exchange between electrons and lattice are taken into account in simulation model. The mechanisms of material removal and the thermodynamic states of matter during laser ablation are studied.

The model system contains 10592 Ni atoms. The atoms interact with one another through Morse potential[1]. In order to shorten the time spent in force calculations, Velocity-Verlet algorithm and Verlet neighbor list[2] have been used.

The initial velocities of atoms are given randomly with a Gaussian distribution at 300 K and follow the Maxwellian distribution in thermal equilibrium state through thermalizing for 50 ps before laser heating. The ideal Maxwellian velocity distribution and the velocity distribution at thermal equilibrium are shown in Fig. 1, where the two velocity distributions are in good agreement with each other and the initial array model proves to be fully acceptable.

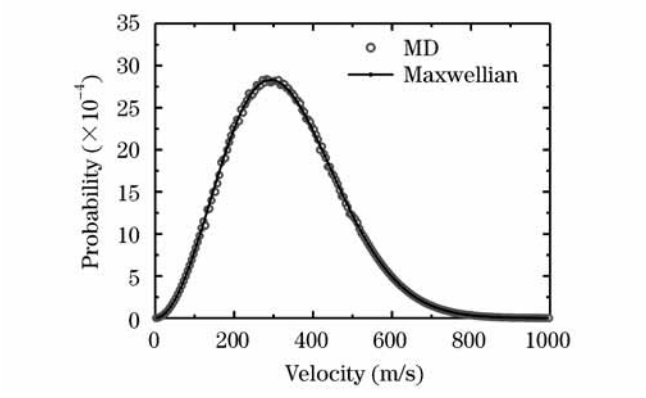

Fig. 1. Velocity distribution of Ni atoms in thermal equilibuium state at 300 K.

Periodic boundary conditions are applied in the x and y directions. A novel and simple velocity-reducing technique is used on the bottom of the simulation model, which can not only avoid spallation at the back side of the target caused by the reflection of stress wave but also ensure efficient ablation.

Under femtosecond laser pulse irradiation, a state of thermal nonequilibrium with electrons and lattice having different temperatures is created, which leads to the different ablation physics from conventional long-pulse laser ablation, namely non-thermal ablation. The processes of laser energy transferring to metals are described by combining the motional equation of each atom with two-step radiation heating model developed by Qiu[3]. As the heat capacity of lattice is rather lower in comparison with that of electrons, the thermal conductivity in the lattice system is neglected. The expressions of model are

$$C_{\mathrm{e}}\frac{\partial T_{\mathrm{e}}}{\partial t} = k_{\mathrm{e}}\frac{\partial^2 T_{\mathrm{e}}}{\partial z^2} - \Phi + Q(z,t), \tag{1}$$

$$C_{\mathrm{a}}\frac{\partial T_{\mathrm{a}}}{\partial t} = \Phi = g(T_{\mathrm{e}} - T_{\mathrm{a}}), \tag{2}$$

where $Q(z,t)$ is the heat flux, C_{e} and C_{a} are the heat capacities (per unit volume) of the electron and the lattice subsystems, K_{e} is the electron thermal conductivity, g is the electron-phonon coupling constant.

Equation (1) is solved by finite difference method to obtain temperature distribution of electrons $T_{\mathrm{e}}(z,t)$ simultaneously with MD integration of the equations of atoms motion. The time step used in the finite difference integration can be estimated based on von Neumann stability criterion

$$\Delta t_{\mathrm{FD}} \leq 0.5(\Delta x_{\mathrm{FD}})^2 C_{\mathrm{e}}(T_{\mathrm{e}})/K_{\mathrm{e}}. \tag{3}$$

As a result, the time steps for two integrations are chosen as 0.25 and 2 fs respectively in simulations.

Laser energy absorption is achieved by adding a velocity-proportional force to the equation of each atom[4]

$$m_i\ddot{r}_i = F_i + \xi m_i v_i, \tag{4}$$

$$\xi = (g/C_a)[(T_e - \langle T_a\rangle)/\langle T_a\rangle], \tag{5}$$

where $\langle T_a\rangle$ is obtained from the atom kinetic energies by averaging the simulation trajectories over several MD time steps in local area. Different from Eq. (5), another expression of ξ is used in the simulations

$$\xi = (g/C_a)(T_e - T_a)/T_a, \tag{6}$$

where T_a is the local temperature of each MD time step and is not equal to $\langle T_a\rangle$ in Eq. (4). The constants used in the simulations are as follows. For Ni, $C_e = \gamma T_e$ with γ= 1065 J/(m^{3}K^2), $C_a = 4.1\times10^6$ J/(m^{3}K), $g = 3.6\times10^{17}$ W/(m^{3}K), $K_e = 91$ W/(m·K). Laser energy absorbed by atoms in a system contributes to increase of kinetic energy.

The simulations are started out with laser fluence of 285 mJ/cm^2. Figure 2 displays the temperature distribution in the top 45 nm of the target from the MD simulations, the negative value of depth represents the region of thermal expansion. It can be seen from Fig. 2 that a small temperature gradient exists at the end of laser pulse and becomes more and more steeper before 10 ps, which is in consequence of a rapid transfer of the absorbed energy to the lattice due to thermal transport by free electrons and strong electron-phonon coupling. At 35 ps, there is a peak at the depth of around 7 nm owing to the transformation of potential energy into kinetic energy in local region and a decrease in the number of atoms, which indicates that a spallation will occur.

During laser-material interaction, a stress wave is produced and propagates into the irradiated material. Figure 3 compares the peak locations of stress wave and longitudinal wave in Ni at different times. Based on the

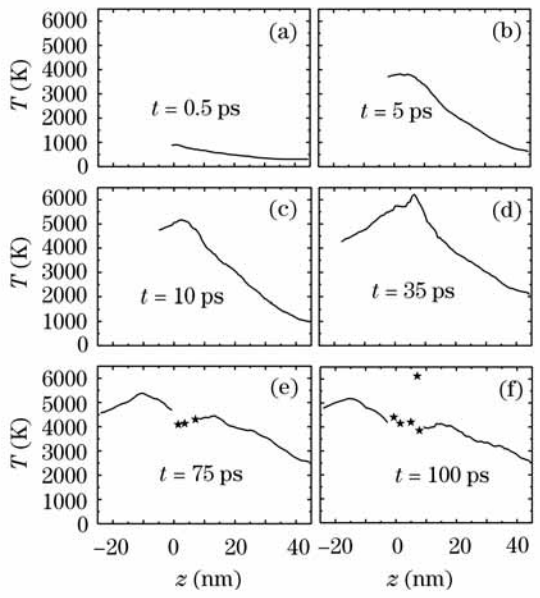

Fig. 2. The temperature distribution of lattice.

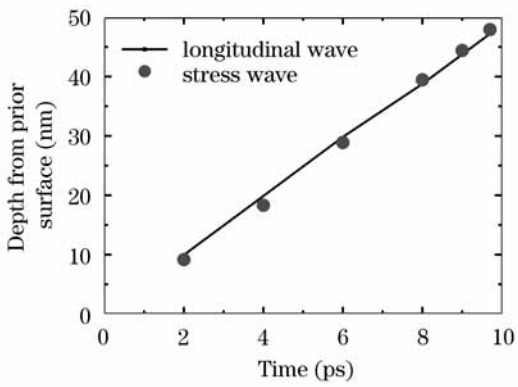

Fig. 3. Propagation of the stress wave and the longitudinal wave.

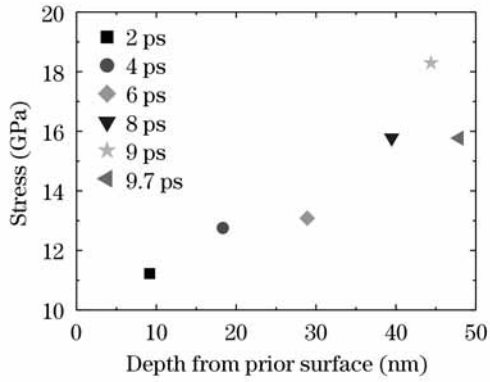

Fig. 4. Transition with times of peak position of stress wave.

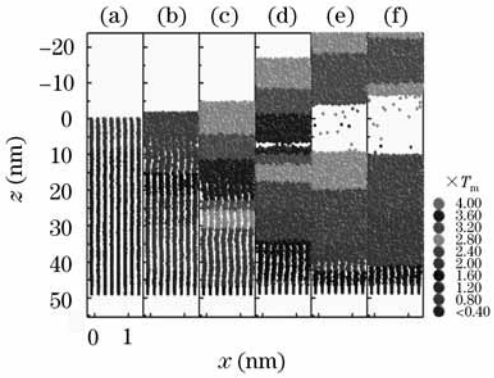

Fig. 5. Snapshots of laser ablation of Ni at fluence of 285 mJ/cm^2. (a): t = 0.5 ps; (b): t = 5 ps; (c): t =10 ps; (d): t = 35 ps; (e): t = 75 ps; (f): t = 100 ps.

locations of the peak at different times, the velocity of stress wave in depth can be predicted. It is seen that the velocity of stress wave is nearly equal to sound velocity, which is c_0 = 4927 km/s for a longitudinal wave in Ni.

The peak values of stress wave at different times are shown in Fig. 4, where stress is calculated from the virial and the compressive stress is denoted by positive value. The peak values of stress wave are increasing before 9 ps, and then attenuate as a result of the release wave, which is increasing with depth under the surface in the course of propagating into the target.

The snapshots from MD simulations of laser irradiation Ni are shown in Fig. 5, the atoms are represented by different gray levels based on local temperature in units of melting point of Ni, T_m = 1728 K. As seen in

the figure, ablation products consist of both individual atoms and a big cluster. Firstly, a big cluster breaks off from the targets. The reason for cluster ejection is that the interaction of the incident release wave corresponding to the unloading of the front face and the reflected stress wave that generates tensile stresses exceeding the strength of the material. A noticeable number of atoms are ejected in succession because of thermal fluctuations in the kinetic energy, which indicates that an intensive thermal evaporation is the reason for individual atoms ejection.

As laser heating progresses, the atoms vibrate more intensively due to the increase of kinetic energy and melting starts from surface of the target. The depth of molten zone can be determined by snapshots and the number density of atoms. In the molten zone, the atomic configuration is destroyed and replaced by random distribution; the number density is also less compared with that of solid. Figure 6 shows the relationship between the depth of molten zone and time, from which a trend of increase with time for the melting depth can be seen. At 5 ps, the melting depth is about 5 nm and increases to 18 nm at 10 ps according to Figs. 6 and 7. However, the temperature of the top 31 nm except molten zone is greatly above $T_{\rm m}$ at this time and can still keep its crystalline structure, which indicates that superheating occurs.

In order to investigate the ablation characteristics at high laser fluences, several fluences above 285 mJ/cm^2 are taken in the simulations. It can be concluded that the ablation characteristics at different fluences have much in common except the number of ejected clusters. Figure 8 gives the snapshots of laser irradiation Ni with a fluence of 400 mJ/cm^2. Compared with Fig. 5, the target tears at several locations, leading to a higher ablation yield of 21 nm/pulse. The rates of ablation at different fluences

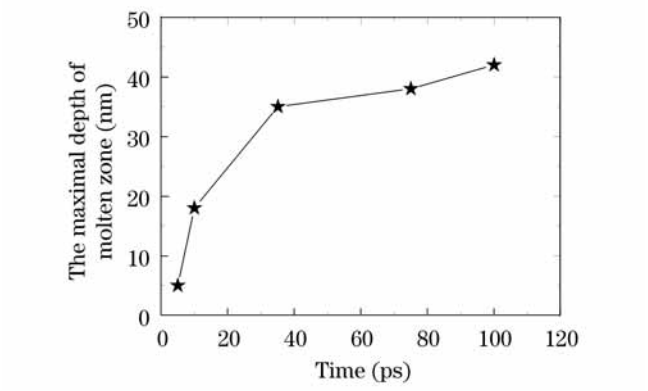

Fig. 6. The depth of molten zone at different times.

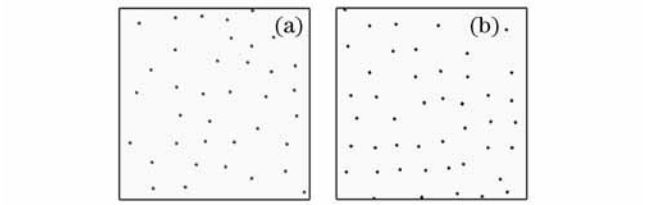

Fig. 7. In-plane structure at different depths. (a): t = 5 ps, z = 5 nm; (b): t = 10 ps, z = 18 nm.

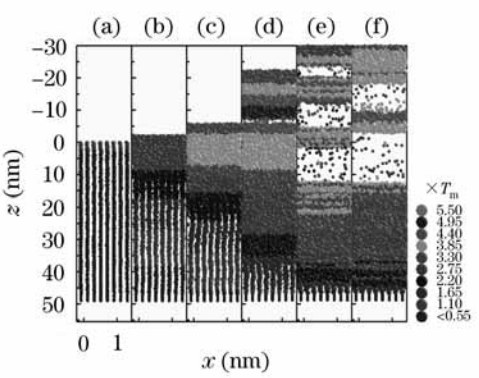

Fig. 8. Snapshots of laser ablation of Ni at fluence of 400 mJ/cm^2. (a): t = 0.5 ps; (b): t = 5 ps; (c): t =10 ps; (d): t = 32 ps; (e): t = 75 ps; (f): t = 100 ps.

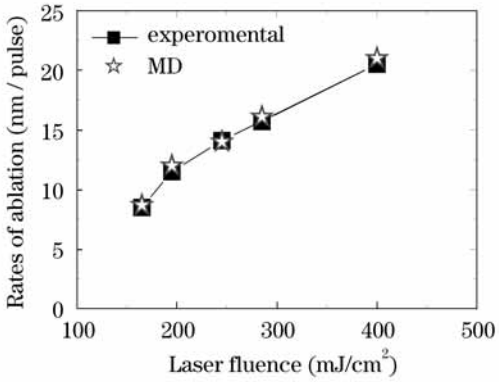

Fig. 9. The rates of ablation at different fluences.

are shown in Fig. 9, which is in good agreement with the experimental data[5].

In conclusion, the dynamics of femtosecond laser ablation of Ni is investigated by means of MD method combined with two-step radiation heating model. Atoms are ablated during non-thermal processes, and the main mechanisms of ablation are found to be evaporation as well as tensile stresses generated inside the target by analyzing the simulation results. The velocity of stress wave is predicted to be nearly equal to sound velocity. Superheating phenomenon is observed. The rates of ablation at different fluences obtained from MD simulations are in good agreement with the experimental data, which proves the availability of simulation methods.

X. Liu's e-mail address is liuxuan@hit.edu.cn.

References

1. L. A. Girifalco and V. G. Weizer, Phys. Rev. **114,** 687 (1959).
2. W. C. Swope, H. C. Anderson, P. H. Berens, and K. R. Wilson, J. Chem. Phys. **76,** 637 (1982).
3. T. Q. Qiu and C. L. Tien, J. Heat Transfer **115,** 835 (1993).
4. H. Häkkinen and U. Landman, Phys. Rev. Lett. **71,** 1023 (1993).
5. S. Preuss, A. Demchuk, and M. Stuke, Appl. Phys. A **61,** 33 (1995).